1-2022

Expression and Purification of a Cleavable Recombinant Fortilin from *Escherichia coli* for Structure Activity Studies

Maranda S. Cantrell
Boise State University

Jackson D. Wall
Boise State University

Xinzhu Pu
Boise State University

Matthew Turner
Boise State University

Luke Woodbury
Boise State University

See next page for additional authors

Publication Information

Cantrell, Maranda S.; Wall, Jackson D.; Pu, Xinzhu; Turner, Matthew; Woodbury, Luke; Fujise, Ken; . . . and Warner, Lisa R. (2022). "Expression and Purification of a Cleavable Recombinant Fortilin from *Escherichia coli* for Structure Activity Studies". *Protein Expression and Purification, 189*, 105989. https://doi.org/10.1016/j.pep.2021.105989

Protein Expression and Purification 189 (2022) 105989

Contents lists available at ScienceDirect

Protein Expression and Purification

journal homepage: www.elsevier.com/locate/yprep

Expression and purification of a cleavable recombinant fortilin from *Escherichia coli* for structure activity studies

Maranda S. Cantrell [a,b], Jackson D. Wall [b], Xinzhu Pu [c], Matthew Turner [c], Luke Woodbury [c], Ken Fujise [d], Owen M. McDougal [b], Lisa R. Warner [b,*]

[a] Biomolecular Sciences Ph.D. Program, Boise State University, Boise, ID, 83725, USA
[b] Department of Chemistry and Biochemistry, Boise State University, Boise, ID, 83725, USA
[c] Biomolecular Research Center, Boise State University, Boise, ID, 83725, USA
[d] Harborview Medical Center, University of Washington, Seattle, WA, 98104-2499, USA

ARTICLE INFO

Keywords:
Fortilin
Translationally controlled tumor protein
Atherosclerosis
Protein expression
Protein purification
NMR spectroscopy
Protease cleavage

ABSTRACT

Complications related to atherosclerosis account for approximately 1 in 4 deaths in the United States and treatment has focused on lowering serum LDL-cholesterol levels with statins. However, approximately 50% of those diagnosed with atherosclerosis have blood cholesterol levels within normal parameters. Human fortilin is an anti-apoptotic protein and a factor in macrophage-mediated atherosclerosis and is hypothesized to protect inflammatory macrophages from apoptosis, leading to subsequent cardiac pathogenesis. Fortilin is unique because it provides a novel drug target for atherosclerosis that goes beyond lowering cholesterol and utilization of a solution nuclear magnetic resonance (NMR) spectroscopy, structure-based drug discovery approach requires milligram quantities of pure, bioactive, recombinant fortilin. Here, we designed expression constructs with different affinity tags and protease cleavage sites to find optimal conditions to obtain the quantity and purity of protein necessary for structure activity relationship studies. Plasmids encoding fortilin with maltose binding protein (MBP), 6-histidine (6His) and glutathione-S-transferase (GST), N- terminal affinity tags were expressed and purified from *Escherichia coli (E. coli)*. Cleavage sites with tobacco etch virus (TEV) protease and human rhinovirus (HRV) 3C protease were assessed. Despite high levels of expression of soluble protein, the fusion constructs were resistant to proteinases without the inclusion of amino acids between the cleavage site and N-terminus. We surveyed constructs with increasing lengths of glycine/serine (GGS) linkers between the cleavage site and fortilin and found that inclusion of at least one GGS insert led to successful protease cleavage and pure fortilin with conserved binding to calcium as measured by NMR.

1. Introduction

Atherosclerosis, or the hardening and narrowing of arterial walls, is the leading cause of death worldwide [1]. Atherosclerogenesis occurs when low density lipoproteins (LDL) in plasma diffuse into the intima of arteries and then become oxidized (oxLDL), followed by uptake into macrophages. Macrophages eventually form foam cells, which over time develop into plaques on the arteries, leading to blockages in blood flow that cause cardiac events such as infarction, stroke, hypertension, etc. Presently, medications used to treat atherosclerosis largely depend on inhibiting the formation of cholesterol *in vivo* via the use of statins, which can cause undesirable side effects. For example, HMG-CoA reductase inhibitors (statin drug class) can cause leg cramps in patients at night that lead to decreased compliance with treatment [2]. Additional side effects may include cataracts and short-term memory loss [3]. Moreover, a recent study of 136,905 people showed that nearly half of all patients brought into the emergency room with heart attacks had normal to low LDL levels in their blood [4]. This finding made evident the need to develop drugs that target other mechanisms in the pathology of atherosclerosis than the *in vivo* formation of high cholesterol.

Fortilin is a promising drug target to treat atherosclerosis [5]. Also known as translationally controlled tumor protein (TCTP) or histamine releasing factor (HRF), fortilin is a highly conserved anti-apoptotic protein [6]. Fortilin consists of 172 amino acids and is found throughout the human body; in the cytosol, nucleus, and mitochondria of all cell types, blood and extracellular space [7,8]. Fortilin exerts its

* Corresponding author. 1910 University Dr, Boise, ID, 83725.
E-mail address: lisawarner@boisestate.edu (L.R. Warner).

https://doi.org/10.1016/j.pep.2021.105989
Received 18 June 2021; Received in revised form 11 September 2021; Accepted 4 October 2021
Available online 6 October 2021

Abbreviations

IPTG	isopropyl-β-*d*-1-thiopyranogalactoside
TEV	tobacco etch virus
HRV 3C	human rhinovirus 3C protease
MBP	maltose binding protein
GST	glutathione-S-transferase
6His	6-histidine
OSM	oncostatin M
NMR	nuclear magnetic resonance
SMI	small molecule inhibitor
TCTP	translationally controlled tumor protein
HRF	histamine release factor
LDL	low density lipoprotein
oxLDL	oxidized LDL
PRX-1	peroxiredoxin-1
PTM	posttranslational modification
LB	Luria Bertani
PBS	phosphate buffered saline
CV	column volume

anti-apoptotic effect through multiple mechanisms including calcium complexation and p53 inactivation, but it contributes to atherosclerosis by keeping macrophages in the M1 pro-inflammatory phenotype [5,9]. Fortilin has been implicated in the progression of atherosclerosis by reducing macrophage apoptosis by binding to and inhibiting p53, a transcription factor that regulates the transcription of BAX, a pro-apoptotic protein. This mechanism promotes foam cell formation, leading to deposits on arterial walls [9]. Fortilin also exhibits anti-apoptotic activity by scavenging free calcium in the cytoplasm of cells, thus exerting a protective effect from calcium-induced apoptosis [10]. Specifically, inhibition of the pro-survival activity of could provide an orthogonal strategy to treat atherosclerosis by shutting down the protective effects of fortilin.

Fortilin is a 19 kDa protein that has 11 beta-strands and an extended flexible loop between residues Arg36 and Ile67 (Fig. 1A). The amino- and carboxy-termini are in proximity to one another, creating a cavity that could be interrogated for small molecule binding. The calcium binding site is coordinated by six oxygen atoms within the beta barrel among residues N131, Q133, L149 and D150 (Fig. 1B) [11]. While a direct connection between fortilin, calcium scavenging, and atherosclerosis has not yet been made, calcium-dependent apoptosis does occur during ox-LDL-induced apoptosis and it is hypothesized that fortilin could play a role through its calcium scavenging activity [12].

A structure-based approach to targeting fortilin will provide important information for drug screening and defining drug binding sites. Structure-based drug design (SBDD) is a technique commonly used to create small molecule therapeutics that specifically target a given protein [13,14]. Solution nuclear magnetic resonance spectroscopy (NMR) is an excellent tool for SBDD, for example, in screening small molecule inhibitors (SMIs), mapping binding hot spots, and determining binding affinities and kinetics [14]. A solution structure of recombinant fortilin has been reported using NMR [11]. Feng et al., used a construct with a 6His affinity tag and required high salt (200 mM) conditions for high quality NMR spectra.

NMR experiments require milligram quantities of pure, isotopically enriched, and bioactive protein. *E. coli* expression platforms are routinely used as they allow for straightforward, high yield and affordable isotope enrichment. Affinity tags are often used for protein purification [15]. Ideally, the affinity tags should be removed by enzymatic cleavage to ensure no pseudo binding effects due to the presence of the affinity tag. The N- and C-termini of fortilin form a beta strand that forms a pocket in the native fortilin structure. Affinity tags attached at either the N- or C-terminus complicate the potential to target this site. Functional studies of fortilin with an affinity tag are inconclusive due to the presence of the affinity tag at the suspected site of small molecule binding site [16,17]. Here, we describe the design and assessment of several fortilin constructs for the purpose of expressing and purifying a recombinant fortilin molecule with minimal non-native residues. Inclusion of a short GGS linker between an HRV 3C protease cleavage site and the N-terminus of fortilin resulted in milligram quantity of isotopically enriched ^{15}N GGS-fortilin. Calcium binding was observed by NMR titrations, demonstrating the structure and activity of this construct were maintained. The work presented here shows that pure recombinant fortilin can be proteolytically cleaved from an affinity tag and retain biological activity by the insertion of a GGS linker sequence.

2. Results and discussion

Initial efforts to produce recombinant tag-less fortilin were hindered by low or no cleavage with either TEV or HRV 3C proteases directed at

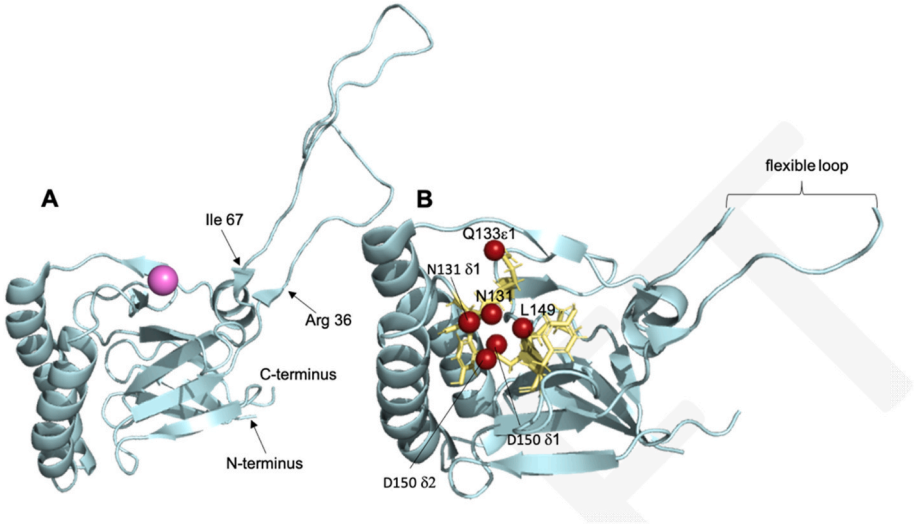

Fig. 1. Calcium-bound fortilin. A) Side view of fortilin (blue) bound to calcium (magenta) with residues labeled for the flexible loop, the N- and C-termini, and B) downward view of fortilin bound to calcium with complexed oxygen atoms (red) shown and residues in proximity displayed as sticks. (For interpretation of the references to colour in this figure legend, the reader is referred to the Web version of this article.)

N-terminal cleavage sites with either 6His, maltose binding protein (MBP), glutathione-S-transferase, or 6His-MBP affinity tag constructs (Fig. 2). Observed cleavage efficiencies for these constructs led to development of a systematic approach to define a minimal linker length required for effective and efficient affinity tag removal.

2.1. Expression and purification of recombinant human fortilin

Each fortilin construct was made using the ATUM pD441 T5 IPTG inducible promoter system. For each of the constructs used, soluble and high purity quantities from 100 mL LB cultures grown at 37 °C were successful. After affinity chromatography using glutathione agarose to purify the $(GGS)_N$ constructs, GST-$(GGS)_N$-fortilin was purified typically with some GST protein made during the protein expression process (SI. Figs. 1–3, 5). For cleavage analysis, the cleaved fortilin construct was compared to the un-cleaved construct, so we decided not to purify further than affinity chromatography for this reason. The same occurred with the MBP-containing constructs where some MBP protein was eluted during affinity chromatography with the desired purified protein (SI. Figs. 4 and 6). Samples containing pure MBP construct were combined and concentrated to workable small volumes for cleavage with either TEV or 3C protease. For the initial cleavage analysis, all constructs were grown at smaller culture volumes (100 mL) to save on materials. The construct we decided to use for NMR titration analysis was the GST-GGS-fortilin construct because cleavage with 3C protease provided the fewest amino acids remaining at the N-terminus of the protein, leaving only GGS-fortilin (SI. Fig. 7). The yield from a 1 L, ^{15}N-labeled culture was 2.08 mg by a reading of the A_{280} and an ε value of 0.595 $(mL/mg)^{-1}$ cm^{-1}. This was an ideal amount for an approximately 200 μM sample for NMR titration analysis.

2.2. Protease cleavage sites distal to fortilin increases MBP removal effectiveness

After treatment of up to 48 h with TEV protease, there was no evidence by SDS-PAGE that the 6His-TEV-fortilin exhibited any cleavage (Fig. 4, lanes 7–10). Next, MBP-TEV-fortilin was treated TEV protease for up to 48 h at room temperature, with again no evidence of cleavage (Fig. 3, lanes 9–12). A construct consisting of 6His-MBP-10N–3C-TEV-fortilin treated with TEV again showed no evidence of cleavage (Fig. 3, lanes 4 and 7). TEV activity was validated with a positive control of MBP-TEV-OSM, or Oncostatin M, a construct known to cleave successfully upon addition of TEV protease [18]. Interestingly, the 6His-MBP-10N–3C-TEV-fortilin construct contained an 3C HRV protease cleavage site distal to the N-terminal site that was left intact after cloning in the TEV site. Treatment with 3C resulted in 72% cleavage after 24 h with no further cleavage after 48 h (Fig. 3, lanes 5 & 8).

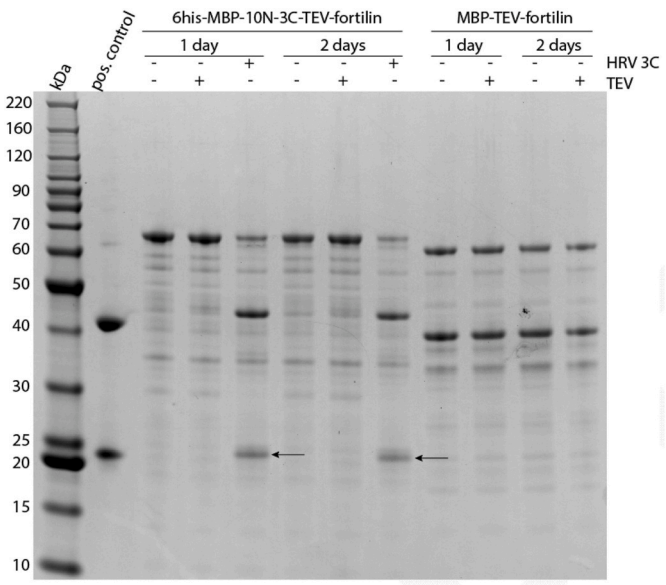

Fig. 3. MBP construct cleavage reactions. SDS-PAGE gel of TEV and 3C protease cleavage reactions. Cleavage reactions of MBP constructs against a positive control lane of MBP-TEV-OSM. Uncleaved MBP-TEV-fortilin can be seen to appear at approximately 62 kDa on a 4–12% SDS-PAGE gradient gel. A band at 42 kDa indicates the MBP affinity tag, presumably due to abortive translations for the MBP-TEV-fortilin construct. Arrows indicate successfully cleaved TEV-fortilin.

2.3. Protease cleavage sites distal to fortilin increases GST removal effectiveness

The GST-3C-TEV-fortilin construct showed no cleavage after two days of incubation with TEV protease (day 2 data not shown). However, upon incubation with HRV 3C protease, cleavage was observed after 24 h. TEV-fortilin is indicated by an arrow in Fig. 4. No cleavage was observed for the 6His-TEV-fortilin construct upon addition of TEV protease after 48 h of incubation at room temperature. The 6His-TEV-fortilin band was confirmed by mass spectrometry, demonstrating no cleavage.

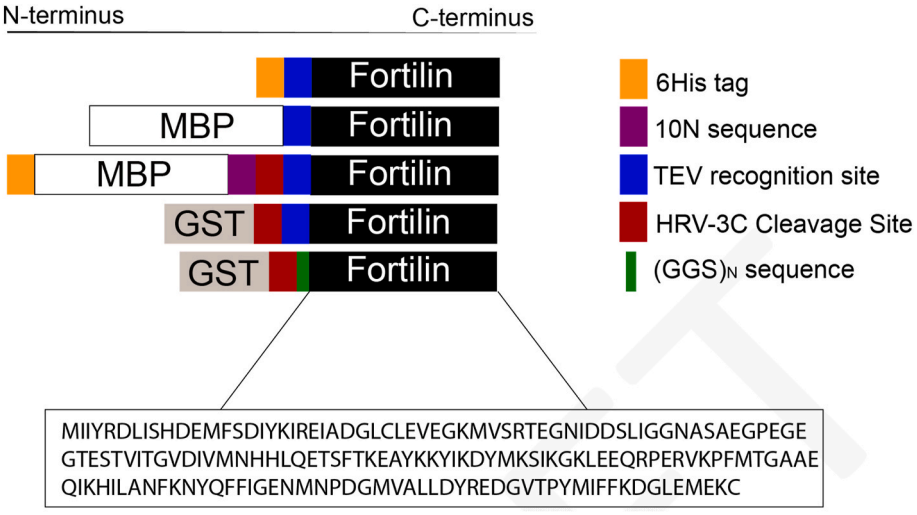

Fig. 2. Constructs used for recombinant fortilin expression, purification, and cleavage. All constructs were made in ATUM's pD441-SR vector.

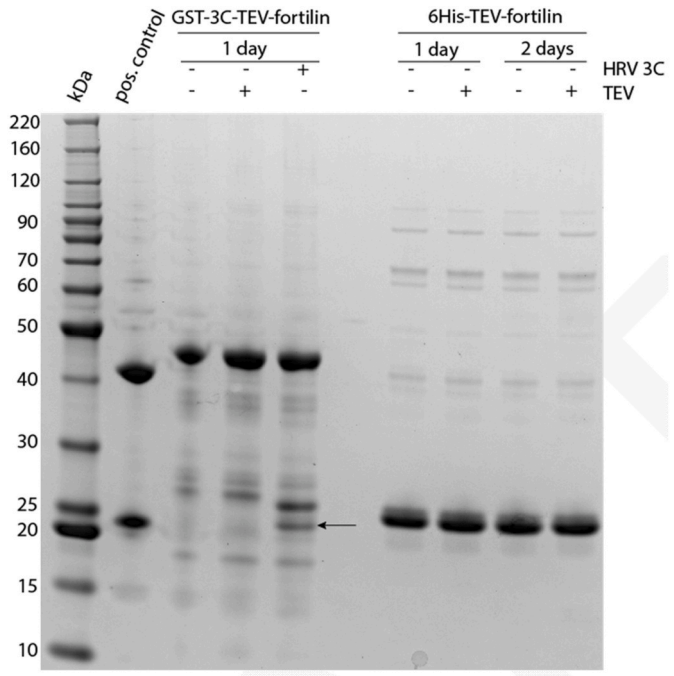

Fig. 4. Protease cleavage sites located proximal to the N-terminus are resistant to cleavage. Cleavage reactions of GST and 6His constructs against a positive control lane of MBP-TEV-OSM. Protein ladder is shown in the first lane to indicate molecular weight markers on a 4–12% bis-acrylamide gradient SDS gel. The arrow indicates successfully cleaved TEV-fortilin, where the 3C cleavage site is N-terminal to the TEV protease cleavage site.

2.4. A minimum GGS tripeptide is required for efficient protease cleavage

It is well-documented that affinity tags can introduce steric hindrance, making the enzymatic cleavage less efficient. Further, the 6His-MBP-10N–3C-TEV-fortilin construct has an additional Human 3C rhinovirus protease cleavage site N-terminal to the TEV cleavage site. Treatment of the 6His-MBP-10N–3C-TEV-fortilin with 3C protease after 24 h at 4 °C resulted in 72% cleaved fortilin. However, this construct was undesirable because it left additional 3C (Leu-Glu-Val-Leu-Phe-Gln-Gly-Pro) and TEV (Glu-Asn-Leu-Tyr-Phe-Gln-Gly-Ser) amino acids; further, there was no additional cleavage observed after 48 h. These observations led us to hypothesize that for efficient cleavage, a linker was needed between the protease cleave site and the fortilin protein.

We systematically investigated what minimum linker length was required for efficient protease cleavage. We used $(GGS)_N$ linker sequences where N = 0, 1, 2 or 3. We found that the inclusion of just one GGS linker sequence $(GGS)_1$ led to cleaved fortilin with the sequence GGS-fortilin; this result was verified against a negative control of $(GGS)_0$, as well as no addition of HRV 3C protease. While additional linker sequences proved successful, we moved forward with $(GGS)_1$-fortilin for NMR analysis to minimize N-terminal binding interference by tag amino acids.

Incorporating a Gly-Gly-Ser (GGS) linker between the protease cleavage site and fortilin increased enzymatic protease cleavage efficiency. We chose to incorporate a repeating GGS motif between the protease cleavage site and fortilin. GGS motifs were chosen for their flexibility, experimentally determined random coil behavior, and charge neutrality [19,20]. GGS linker units were either not included in the construct $(GGS)_0$ or included in increasing repeats of GGS from $(GGS)_1$ to $(GGS)_3$. Addition of just one GGS linker to the N-terminus of fortilin was sufficient to produce a successfully cleaved construct, with approximately 86.5% cleavage GGS-fortilin after treatment with 3C protease (Table 1). Addition of two GGS linker sequences provided 81.5% cleavage, and addition of three GGS linkers resulted in 85% cleavage efficiency. Confirmation of cleavage reactions was analyzed by SDS-PAGE (Fig. 5) and compared to a positive control of GST-3C-Syk protein to ensure protease activity. All samples were also compared against negative controls wherein no protease was added. Addition of extra $(GGS)_N$ linkers showed no increase in cleavage efficiency. Addition of one GGS linker sequence at the N-terminus of fortilin appeared to have provided sufficient access for a protease to cleave the affinity tag from fortilin for biological studies. Recovery yields after protease cleavage are available in Table 1. Yields were quantified in comparison to the respective non-cleaved construct on the same SDS gel.

Table 1
Percent yield of tag free fortilin after one day to cleave constructs. Yields quantified using SDS PAGE image analysis using GelAnalyzer [21].

Construct	Cleaved construct	Percent (%) recovery of cleaved fortilin
6His-TEV-fortilin	fortilin	0
6His-MBP-10N–3C-TEV-fortilin	TEV-fortilin	72
GST-3C-TEV-fortilin	TEV-fortilin	28
GST-3C-$(GGS)_0$-fortilin	fortilin	0.5
GST-3C-$(GGS)_1$-fortilin	GGS-fortilin	86.5
GST-3C-$(GGS)_2$-fortilin	$(GGS)_2$-fortilin	81.5
GST-3C-$(GGS)_3$-fortilin	$(GGS)_3$-fortilin	85

2.5. Calcium titration of $(GGS)_1$-fortilin

It is well established that fortilin binds to calcium and the binding site has been characterized (see Fig. 1) [11,22,23]. For the present study, we reproduced $CaCl_2$ titration analysis with the ^{15}N-labeled $(GGS)_1$-fortilin protein using NMR spectroscopy and obtained a K_d value of 13 μM, which is within reason to previously reported affinities of fortilin for Ca^{2+} [11]. Multiple literature reports provide the K_d values for calcium binding to fortilin that range from 10 μM to 17.5 μM to 22 mM and 25 mM [10,11,24]. The present study shows that recombinant fortilin, in the absence of an affinity tag, still binds calcium. Biologically, fortilin binds calcium to mediate histamine release from basophils, which play a critical role in immune system function [6].

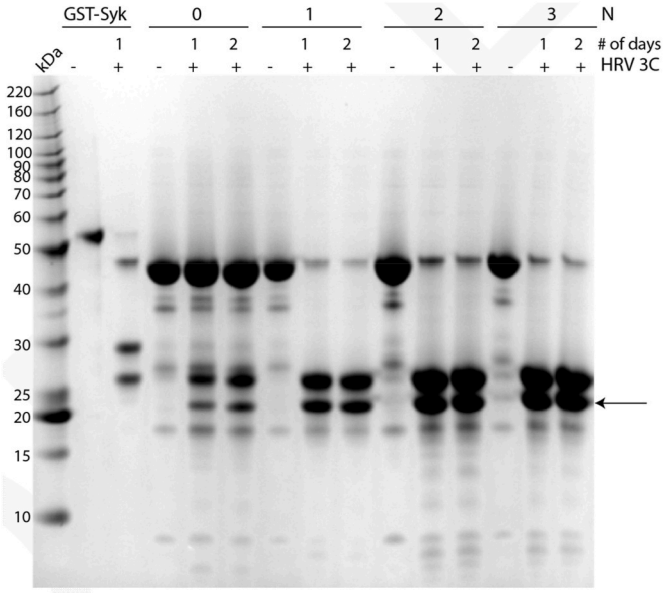

Fig. 5. Cleavage reactions of $(GGS)_N$ constructs where N = 0, 1, 2 or 3 against a positive control lane of cleaved GST-3C-Syk. Protein ladder is shown in the first lane to indicate molecular weight markers on a 4–12% polyacrylamide SDS gradient gel. Arrow indicates successfully cleaved $(GGS)_N$-fortilin that was confirmed by mass spectrometry.

A 1 M aqueous solution of calcium chloride ($CaCl_2$) was titrated into a solution of 176 μM $(GGS)_1$-fortilin. Aliquots of 1 μL $CaCl_2$ were used for each titration point for a total of 6 points. Notable peak shifts in the titration can be seen in Fig. 6 where arrows indicate increasing concentrations of $CaCl_2$. The combined chemical shifts were calculated for Y132 and a quadratic expansion of the isotherm binding model binding isotherm was fit to the data to yield a binding affinity of K_d of 14 mM ± 3.6 mM.

3. Conclusion

The successful cleavage of the 6His-MBP-10N–3C-TEV-fortilin and GST-3C-TEV-fortilin constructs led us to the hypothesis that, at the N-terminus, space is required for a protease searching for a cleavage recognition sequence to gain access to the cleavage site. Insertion of just one GGS linker sequence, at the N-terminus and before the cleavage site, provided 78% recovery of GGS-fortilin (Fig. 5). Further characterization of this activity needs to be done to determine the mechanism by which native fortilin hinders protease activity at the N-terminus. According to computational ligand docking studies performed by our lab that were consistent with a previous study, the N-terminus is a predicted location for small molecule binders and is required for activity [25,26]. Additionally, the N-terminus has been shown to be highly conserved among various species and is required for anti-apoptotic activity of fortilin both *in vivo* and *in vitro* when binding to Bcl-xL, a protein that is required in cell survival maintenance [26]. This is experimentally backed by previous work published using *Plasmodium falciparum*, where the artemisinin binding site was characterized, and the binding site was near the N-terminus [17]. Indeed, previous computational work published by our lab has shown that fortilin binds peroxiredoxin-1 (PRX-1), a protein implicated in reactive oxygen species (ROS)-mediated apoptosis, near the N-terminus [27]. It should be noted, however, that to date the binding site for artemisinin or dihydroartemisinin (DHA) has not been characterized in human fortilin, while evidence suggests that DHA does bind human fortilin [16,17].

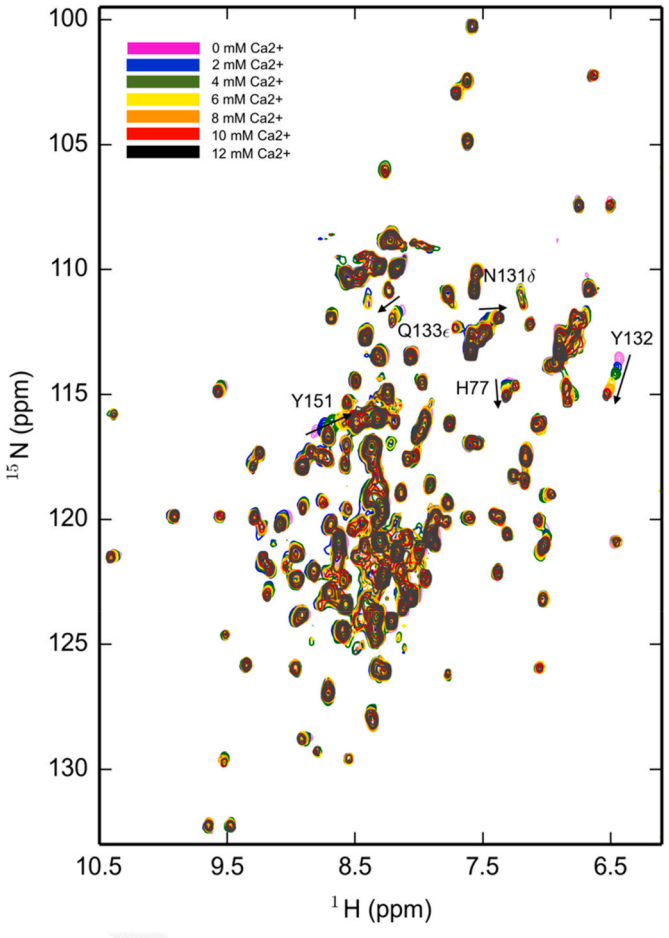

Fig. 6. ^{1}H,^{15}N HSQC spectral overlay of GGS-fortilin titrated with calcium. Y132, Y151, N131, Q133, and H77 are labeled with arrows indicating increasing concentrations of calcium.

The present study has shown that recombinant, pure, isotopically labeled fortilin can be produced with a cleavable affinity tag when just one GGS linker is added to the N-terminus. This indicates that the N-terminus is partially hidden from protease in the absence of the linker sequence. More studies need to be performed to not only determine the mechanism by which addition of a GGS sequence facilitates cleavage, but to also characterize the interaction of small molecules at the N-terminus, such as artemisinin and DHA, which bind but have not been characterized in human recombinant fortilin [16,17]. Additionally, NMR studies need to be performed on fortilin in other expression systems, such as yeast, to explore the possibility of post-translational modifications (PTMs), and to determine the differences in binding between recombinant fortilin products in *E. coli*, *P. pastoris*, and human cell lines.

4. Materials and methods

4.1. Reagents

Unless otherwise mentioned, chemical reagents were purchased from Fisher Scientific (Waltham, MA). Isotopically enriched reagents were purchased from MilliPoreSigma (St Louis, MO).

4.1.1. Expression and purification of S219V TEV protease from E. coli

Recombinant TEV protease was expressed and purified using pRK793 [28] (a gift from David Waugh (Addgene plasmid # 8827; http://n2t.net/addgene:8827; RRID:Addgene_8827)) in BL21 (DE3) strain *E. coli*. From a glycerol stock, 20 mL of Luria Bertani (LB) broth containing 100 μg/mL ampicillin, 25 μg/mL chloramphenicol was inoculated, and incubated overnight at 37 °C with shaking at 200 rpm. This overnight culture was then used to inoculate 1L LB containing 100 μg/mL ampicillin, 25 μg/mL chloramphenicol with shaking at 37 °C with 200 rpm. Once the OD_{600} reached between 0.5 and 0.7, a pre-induction sample equivalent to 1 mL of cells at OD_{600} of 0.8 was collected, and the culture flasks placed on ice and gently rotated every few minutes to cool the cultures. The incubator was then set to 30 °C and the cultures were reintroduced at the elevated temperature and expression was induced with 1 mM IPTG, with shaking at 200 rpm. This culture was incubated overnight. On the third day, a post-induction sample equivalent to 1 mL of cells at OD_{600} of 0.8. The pre- and post-induction samples were used to analyze expression using SDS-PAGE. Lysis was halted by pouring the cultures into pre-weighed 500 mL centrifuge bottles and the cultures centrifuged at 6000×*g* for 30 min at 4 °C. After centrifugation, the supernatants were removed, and the mass of the pelleted bacteria weighed. The pellet was resuspended in 40 mL of lysis buffer consisting of 50 mM Tris-Cl pH 8.0, 300 mM NaCl, 20 mM imidazole, 10% (w/v) sorbitol, 20 mM β−mercaptoethanol, 0.02 mg/mL lysozyme, and 1X HALT protease inhibitors (Thermofisher, USA). The suspension was sonicated on ice water at 60% power, 30 s on/30 s off for 4.5 min of total pulse time and a 75 μl sample collected for SDS-PAGE to check post sonication pellet and supernatant. The sonicated suspension was centrifuged at 16,000×*g* for 30 min at 4 °C. The supernatant was collected and filtered using a 0.45 μm PES filter. To the filtered lysate, 5 mL of Ni-NTA superflow slurry (Qiagen Cat #30410/30,430) was added and the mixture incubated overnight at 4 °C with rocking. On the fourth day, the lysate/resin mix was loaded into a column and the flow through collected. Purification was carried out with a BioLogic LP System using EconoColumn 1.0 × 10 cm chromatography

columns (Bio-Rad, Hercules, CA, USA). To line A, the lysis buffer described previously was attached. To line B, the same lysis buffer with the only difference being a 300 mM imidazole concentration was attached. Buffer A was run over the column at a flow rate of 1.0 mL/min until the A_{280} stabilized, all while collecting the flow through. The program for protein purification was as follows: Line A for 10 min, Line B (0%–100% B, 1.0 mL/min) for 60 min, hold Line B for 10 min, and back to 100% A for 10 min. Results were evaluated by SDS-PAGE. Fractions containing purified TEV protease were combined, and protein concentration determined by absorbance at 280 nm. Pooled fractions were diluted to a final concentration of 1 mg/mL in a 50% glycerol solution, and 0.5 mL aliquots stored at −80 °C.

4.1.2. Expression plasmid constructs

Plasmids were purchased from ATUM (Newark, CA) using their pD441-SR vector. These constructs consisted of glutathione S-transferase (GST), maltose binding protein (MBP), and 6-histidine (6His) affinity tags, human rhinovirus (HRV) 3C and tobacco etch virus (TEV) protease recognition sites, and glycine-glycine-serine (GGS) linkers of varying length $(GGS)_N$ where N = 0, 1, 2 or 3 at the N-terminus of fortilin in the pD441-SR expression vector.

4.1.3. Expression of recombinant fusion proteins

Plasmids were transformed into 50 μL of competent *E. coli* cells using the heat-shock method at 42 °C. Single colonies were inoculated into 5 mL of LB medium containing 50 μg/mL kanamycin and grown at 37 °C overnight with shaking at 250 rpm. One mL of each overnight culture was inoculated into 100 mL LB medium containing 50 μg/mL kanamycin and grown at 37 °C with shaking at 250 rpm until the OD_{600} reached between 0.60 and 0.80. Once reached, IPTG was added to 0.1 mM to induce protein expression. Expression continued at these conditions for 6 h. Cells were harvested by centrifugation at 4,000×*g* for 20 min and expression was assessed by SDS-PAGE on 4–12% bis-acrylamide gradient gels.

4.1.4. Expression of ^{15}N-labeled recombinant fusion proteins for NMR spectroscopy

Plasmids were transformed into 50 μL of competent *E. coli* cells using the heat-shock method at 42 °C. Single colonies were inoculated into 5 mL of LB medium containing 50 μg/mL kanamycin and grown at 37 °C and grown for approximately 8 h. One mL of each culture was inoculated into 50 mL of ^{15}N-labeled M9 minimal media containing 50 μg/mL kanamycin and grown at 37 °C overnight.

4.1.5. Cell lysis

Cell pellets (approximately 0.13 g each) from 100 mL cultures were resuspended in 2 mL lysis buffer containing 1X phosphate buffered saline (PBS), pH 7.4 and 0.1% Triton X-100. Lysozyme was added to a final concentration of 0.25 mg/mL as well as ½ tablet of HALT protease inhibitor cocktail (Pierce, Rockford, IL). The lysate was then subjected to sonication at 70% power for 30 s on/30 s off for a total of 2 min. Samples were then centrifuged at 17,000×*g* for 45 min at 4 °C. The resulting lysate was filtered through a 0.45 μm PES filter and subjected to affinity purification.

4.1.6. Purification of GST-3C-$(GGS)_N$-fortilin and GST-3C-TEV-fortilin from BL21(DE3) cells

GSTrap sepharose 4B 1 mL pre-packed columns were used for purification (GE Healthcare, Marlborough, MA). Separate columns were used for each linker sequence to avoid contamination of samples. Samples were loaded onto the column with a flow rate of 1.0 mL/min and washed with 1X PBS with a flow rate of 1.0 mL/min for 20 mL, followed by a 10 mL elution with GSTrap elution buffer containing 50 mM Tris-HCl pH 8.0 and 10 mM reduced glutathione. Elution was followed by a 10 mL wash at 1.0 mL/min with 1X PBS (Supp. Figs 1-3 and 5). All solutions used for affinity chromatography were filtered through 0.22 μm nylon filters and degassed under vacuum with rigorous stirring for at least 1 h.

4.1.7. Purification of 6His-MBP-10N–3C-TEV-fortilin and MBP-TEV-fortilin

Amylose resin (New England Biolabs, Ipswich, MA) was used for purification of MBP-tagged proteins. An approximately 50% slurry of affinity beads to 20% ethanol were used to pack a column by gravity until the column volume reached 3 mL. The column was equilibrated with 25 mL of column buffer containing 20 mM Tris-HCl pH 7.4, 0.2 M NaCl and 1 mM EDTA. The clarified lysate was added to the column and the flow through collected. This step was repeated once to improve protein binding. Next, the column was washed with 10 column volumes (CV) of the column buffer described above. This was followed by elution by flowing 5 CV of column buffer containing 10 mM maltose, collected over three elution steps. A final wash step of 10 CV column buffer was performed to remove any remaining protein (Supp. Figs. 4 and 6).

4.1.8. Purification of 6His-TEV-fortilin

Nickel agarose resin (HisPur™ Ni-NTA Superflow agarose, (ThermoFisher Scientific, Waltham, MA) was used for purification of 6His-TEV-fortilin. An approximately 50% slurry of affinity beads in 20% ethanol were used to pack a column by gravity until the column volume reached 3 mL. The column was equilibrated with 25 mL of buffer containing 50 mM Tris-Cl pH 8.0, 300 mM NaCl, 20 mM imidazole. Next, the clarified lysate was added to the column and the flow through collected. This step was repeated once to improve binding to the column. The column was then washed with 10 CV of buffer containing 50 mM Tris-Cl pH 8.0, 300 mM NaCl, 20 mM imidazole. This was followed by elution with 5 CV of buffer containing 50 mM Tris-Cl pH 8.0, 300 mM NaCl, 200 mM imidazole (Supp. Fig. 5).

4.1.9. HRV 3C cleavage of affinity tags from fusion proteins and removal of proteases

Samples containing purified fusion protein containing the 3C protease site (LEVLFQ/GP) underwent cleavage with either human rhinovirus 3C (HRV 3C) using the Pierce HRV 3C protease solution kit (Pierce, Rockford, IL) according to manufacture protocols. Protease removal was also done according to manufacture protocols by dialysis using 0.5–3.0 mL capacity dialysis cassettes (ThermoFisher Scientific, Waltham, MA) into 3C cleavage buffer containing 50 mM Tris-Cl pH 7.0, 150 mM NaCl and 1 mM EDTA. Samples were dialyzed and cleaved with 23 μL of the 3C protease at 4 °C; 25 μL of sample was checked for cleavage by SDS-PAGE after 24 and 48 h. For the $(GGS)_1$ construct, the cleaved protein (GGS-fortilin) was buffer exchanged from protease buffer by size exclusion chromatography using an S75 column equilibrated within 100 mM NH_4HCO_3 (Cytiva, Marlborough, MA). Fractions containing pure protein were combined and concentrated using 5 MWCO PES Vivaspin 20 columns (Sartorius, Stonehouse, UK) by centrifugation at 4000×*g* until the volume reached approximately 10 mL. These were then aliquoted such that microcentrifuge tubes contained 2 mg protein each and lyophilized at 2 atm and −80 °C overnight using a LabConco FreeZone 2.5 Plus lyophilizer (LabConco, Kansas City, MO). Samples were stored at −20 °C.

4.1.10. TEV protease cleavage of affinity tags from fusion proteins

Samples containing purified fusion protein containing the tobacco enterovirus (TEV) protease site (ENLYFQ/SG) using in-house grown TEV protease (expression and purification protocol above) using 2 μL protease solution for every 200 μg of protein in the elution buffer according to the corresponding construct. Samples were rotated at room temperature and 25 μL aliquots checked at 24 and 48 h by SDS-PAGE.

4.1.11. SDS-PAGE analysis of protein expression, purification and cleavage

Protein expression, purification and cleavage steps were analyzed using sodium dodecyl sulfate polyacrylamide gel electrophoresis (SDS-

PAGE). Samples were prepared such that equal loading was observed in each gel. Gels were prepared according to standard protocol and used for protein separation with (4–12%) resolving and stacking (6%) gels (Invitrogen, Carlsbad, CA). Quantification was done using GelAnalyzer 19.1 [21].

4.1.12. NMR spectroscopy for activity assay via calcium titration of $(GGS)_N$-fortilin

Lyophilized $(GGS)_N$-fortilin (1.76 mg) was resuspended in 500 μL of a 20 mM tris-Cl buffer, pH 8.0, containing 200 mM NaCl and 10% D_2O. An aqueous 1 M $CaCl_2$ stock solution was used for each titration. Spectra were recorded at 298 K on a Bruker AVANCE III 600 MHz spectrometer equipped with a 5 mm TCI cryoprobe with z-axis gradients. ^1H, ^{15}N HSQC spectra were collected with the Bruker pulse program *hsqcfpf3gpphwg* [29]. Spectra were processed with Topspin 3.2 (Bruker, Billerica, MA), NMRPipe [30] and plotted using NMRglue [31]. For each titrant, 1–2 μL stock $CaCl_2$ was added to a microcentrifuge test tube containing the NMR sample. The sample was then placed into a glass NMR tube, with care taken to avoid air bubbles. This was then placed in the NMR spectrometer and measurements taken. Chemical shift analysis was done using CcpNmr Analysis V3 [32,33]. Binding analysis was performed on the largest chemical shift perturbations (CSPs) using the combined chemical shift difference in both ^{15}N and ^1H [34]. CSPs were then plotted against the concentration of Ca^{2+} delivered and fit to a saturation binding model, given by:

$$\Delta_\delta = \frac{Kd + [L] + [P] - \sqrt{(Kd + [L] + [P])^2 - 4\,[L][P]}}{2\,[P]}\Delta_{\delta max}$$

where Δ_δ is the change in chemical shift upon addition of ligand, [P] is the concentration of fortilin, [L] is the concentration of ligand (or Ca^{2+}), and $\Delta_{\delta max}$ is the maximum chemical change upon saturation of fortilin with Ca^{2+}. Curve fitting and error analysis was performed using Wolfram Mathematica.

4.1.13. LC-MS based proteomics analysis

Proteomic analysis was performed using a method established previously with modifications [35]. Excised gel pieces were de-stained in 50 mM ammonium bicarbonate/50% acetonitrile, reduced in 10 mM DTT for 60 min at 56 °C, and alkylated in 55 mM iodoacetamide for 60 min at room temperature in the dark. Gel pieces were then digested with proteomics grade trypsin (Thermo Fisher Scientific, Waltham, MA) overnight at 37 °C. Resulting peptide mixtures were chromatographically separated on a reverse-phase C_{18} column (10 cm × 75 μm, 3 μm, 120 Å) and analyzed on a Velos Pro Dual-Pressure Linear Ion Trap mass spectrometer (Thermo Fisher Scientific, Waltham, MA) as described previously [35].

Peptide spectral matching and protein identification were achieved by database search using Sequest HT algorithms in Proteome Discoverer 2.2 (ThermoFisher Scientific, Waltham, MA). Raw spectral data were searched against a protein sequence database containing the anticipated sequences and UniProtKB/Swiss-Prot protein database for *E. coli* (acquired from www.uniprot.org on November 3, 2020). Main search parameters included: trypsin, maximum missed cleavage site of two, precursor mass tolerance of 1.5 Da, fragment mass tolerance of 0.8 Da, fixed modification of cysteine carbamidomethylation (+57.021 Da), and variable modification of methionine oxidation (+15.995 Da). Decoy database search was performed to calculate false discovery rate (FDR). Proteins containing one or more peptides with FDR ≤0.01 were considered positively identified and reported.

Data availability

All mass spectrometry data and results are available upon request. Please contact Dr. Shin Pu at shinpu@boisestate.edu and Dr. Maranda Cantrell at marandacantrell@u.boisestate.edu.

Author contributions

Maranda Cantrell: Conceptualization, Methodology, Formal Analysis, Investigation, Data Curation, Writing – Original Draft, and Visualization. Jackson Wall: Methodology and Investigation. Shin Pu: Validation and Investigation. Matthew Turner: Validation and Investigation. Luke Woodbury: Investigation. Ken Fujise. Resources, Supervision, and Funding Acquisition. Owen McDougal: Conceptualization, Resources, Supervision, and Funding Acquisition. Lisa Warner: Conceptualization, Methodology, Formal Analysis, Resources, Visualization, Supervision, and Funding Acquisition. All Authors: Writing – Review and Editing.

Acknowledgements

The authors would like to thank Dr. Joseph DuMais for training and support in the Department of Chemistry and Biochemistry NMR Center. M.S.C. and J.D.W. both gratefully acknowledge support from Sigma Xi Grants-in-Aid of Research, March 2019. The project described was supported in part by NIH grants P20GM103408, P20GM109095, 1C06RR020533, R01HL138992 and the Boise State University Biomolecular Research Center (RRID:SCR_019174) with funding from the National Science Foundation, Grants #0639251 and #0923535; the M. J. Murdock Charitable Trust; Lori and Duane Stueckle, and the Idaho State Board of Education. Its contents are solely the responsibility of the authors and do not necessarily represent the official views of NIH. L.R.W. acknowledges funding for this project in part from Institutional start-up funds from the Department of Chemistry and Biochemistry at Boise State University.

Appendix A. Supplementary data

Supplementary data to this article can be found online at https://doi.org/10.1016/j.pep.2021.105989.

References

[1] E.J. Benjamin, P. Muntner, A. Alonso, M.S. Bittencourt, C.W. Callaway, A. P. Carson, A.M. Chamberlain, A.R. Chang, S. Cheng, S.R. Das, F.N. Delling, L. Djousse, M.S.V. Elkind, J.F. Ferguson, M. Fornage, L.C. Jordan, S.S. Khan, B. M. Kissela, K.L. Knutson, T.W. Kwan, D.T. Lackland, T.T. Lewis, J.H. Lichtman, C. T. Longenecker, M.S. Loop, P.L. Lutsey, S.S. Martin, K. Matsushita, A.E. Moran, M. E. Mussolino, M. O'Flaherty, A. Pandey, A.M. Perak, W.D. Rosamond, G.A. Roth, U. K.A. Sampson, G.M. Satou, E.B. Schroeder, S.H. Shah, N.L. Spartano, A. Stokes, D. L. Tirschwell, C.W. Tsao, M.P. Turakhia, L.B. VanWagner, J.T. Wilkins, S.S. Wong, S.S. Virani, Heart disease and stroke statistics—2019 update: a report from the American heart association, Circulation 139 (2019) e1–e473, https://doi.org/10.1161/CIR.0000000000000659.

[2] J.V. Pergolizzi, F. Coluzzi, R.D. Colucci, H. Olsson, J.A. LeQuang, J. Al-Saadi, P. Magnusson, Statins and muscle pain, Expet Rev. Clin. Pharmacol. 13 (2020) 299–310, https://doi.org/10.1080/17512433.2020.1734451.

[3] A.M. Alsehli, G. Olivo, L.E. Clemensson, M.J. Williams, H.B. Schiöth, The cognitive effects of statins are modified by age, Sci. Rep. 10 (2020) 1–14, https://doi.org/10.1038/s41598-020-63035-2.

[4] A. Sachdeva, C.P. Cannon, P.C. Deedwania, K.A. LaBresh, S.C. Smith, D. Dai, A. Hernandez, G.C. Fonarow, Lipid levels in patients hospitalized with coronary artery disease: an analysis of 136,905 hospitalizations in Get with the Guidelines, Am. Heart J. 157 (2009), https://doi.org/10.1016/j.ahj.2008.08.010.

[5] D. Pinkaew, K. Fujise, Fortilin: a potential target for the prevention and treatment of human diseases, Adv. Clin. Chem. 82 (2017) 265–300, https://doi.org/10.1016/bs.acc.2017.06.006.

[6] S.M. MacDonald, Potential role of histamine releasing factor (HRF) as a therapeutic target for treating asthma and allergy, J. Asthma Allergy (2012) 51–59, https://doi.org/10.2147/JAA.S28868.

[7] F. Li, D. Zhang, K. Fujise, Characterization of fortilin, a novel antiapoptotic protein, J. Biol. Chem. 276 (2001) 47542–47549, https://doi.org/10.1074/jbc.M108954200.

[8] U.A. Bommer, A. Telerman, Dysregulation of TCTP in biological processes and diseases, Cells 9 (2020) 1–19, https://doi.org/10.3390/cells9071632.

[9] K. Fujise, D. Pinkaew, M. Eltorky, R.J. Le, Y. Chen, B. Teng, Fortilin reduces apoptosis in macrophages and promotes atherosclerosis, Am. J. Physiol. Cell Physiol. 305 (2013) H1519–H1529, https://doi.org/10.1152/ajpheart.00570.2013.

[10] K. Fujise, P. Graidist, A. Nakatomi, M. Yazawa, A. Phongdara, J. Chang, C.C.-J. Lin, M. Tonganunt, Fortilin binds Ca 2+ and blocks Ca 2+ -dependent apoptosis in vivo, Biochem. J. 408 (2007) 181–191, https://doi.org/10.1042/bj20070679.
[11] Y. Feng, D. Liu, H. Yao, J. Wang, Solution structure and mapping of a very weak calcium-binding site of human translationally controlled tumor protein by NMR, Arch. Biochem. Biophys. 467 (2007) 48–57, https://doi.org/10.1016/j.abb.2007.08.021.
[12] C. Vindis, M. Elbaz, I. Escargueil-Blanc, N. Auge, A. Heniquez, J.C. Thiers, A. Nègre-Salvayre, R. Salvayre, Two distinct calcium-dependent mitochondrial pathways are involved in oxidized LDL-induced apoptosis, Arterioscler. Thromb. Vasc. Biol. 25 (2005) 639–645, https://doi.org/10.1161/01.ATV.0000154359.60886.33.
[13] J.P. Hughes, S.S. Rees, S.B. Kalindjian, K.L. Philpott, Principles of early drug discovery, Br. J. Pharmacol. 162 (2011) 1239–1249, https://doi.org/10.1111/j.1476-5381.2010.01127.x.
[14] A.C. Anderson, The process of structure-based drug design, Chem. Biol. 10 (2003) 787–797, https://doi.org/10.1016/j.chembiol.2003.09.002.
[15] G.L. Rosano, E.A. Ceccarelli, Recombinant protein expression in Escherichia coli: advances and challenges, Front. Microbiol. 5 (2014) 1–17, https://doi.org/10.3389/fmicb.2014.00172.
[16] T. Fujita, K. Felix, D. Pinkaew, N. Hutadilok-Towatana, Z. Liu, K. Fujise, Human fortilin is a molecular target of dihydroartemisinin, FEBS Lett. 582 (2008) 1055–1060, https://doi.org/10.1016/j.febslet.2008.02.055.
[17] W. Li, Y. Zhou, G. Tang, Y. Xiao, Characterization of the artemisinin binding site for translationally controlled tumor protein (TCTP) by Bioorthogonal click Chemistry, Bioconjugate Chem. 27 (2016) 2828–2833, https://doi.org/10.1021/acs.bioconjchem.6b00556.
[18] M.T. Nguyen, M.J. Prima, J.-A. Song, J. Kim, B.H. Do, J. Yoo, S. Park, J. Jang, S. Lee, E. Lee, M. de P. Novais, H.-B. Seo, S. Lee, M.-L. Cho, C.J. Kim, Y.J. Jang, H. Choe, Prokaryotic soluble overexpression and purification of oncostatin M using a fusion approach and genetically engineered E. coli strains, Sci. Rep. 9 (2019) 13706, https://doi.org/10.1038/s41598-019-50110-6.
[19] T.H. Evers, E.M.W.M. Van Dongen, A.C. Faesen, E.W. Meijer, M. Merkx, Quantitative understanding of the energy transfer between fluorescent proteins connected via flexible peptide linkers, Biochemistry 45 (2006) 13183–13192, https://doi.org/10.1021/bi061288t.
[20] W.G. Miller, Random coil configurations of polypeptide copolymers, J. Mol. Biol. 23 (1967) 67.
[21] I. Lazar Jr., I. Lazar Sr, GelAnalyzer 19.1, n.d, http://www.gelanalyzer.com.
[22] J. Bhisutthibhan, M.A. Philbert, H. Fujioka, M. Aikawa, S.R. Meshnick, The Plasmodium falciparum translationally controlled tumor protein: subcellular localization and calcium binding, Eur. J. Cell Biol. 78 (1999) 665–670, https://doi.org/10.1016/S0171-9335(99)80052-1.
[23] M. Kim, Y. Jung, K. Lee, C. Kim, Identification of the calcium binding sites in translationally controlled tumor protein, Arch Pharm. Res. (Seoul) 23 (2000) 633–636, https://doi.org/10.1007/BF02975253.
[24] N.G. Haghighat, L. Ruben, Purification of novel calcium binding proteins from Trypanosoma brucei: properties of 22-,24- and 38-kilodaltion proteins, Mol. Biochem. Parasitol. 51 (1992) 99–110.
[25] D. Pinkaew, A. Chattopadhyay, M.D. King, P. Chunhacha, Z. Liu, H.L. Stevenson, Y. Chen, P. Sinthujaroen, O.M. McDougal, K. Fujise, Fortilin binds IRE1α and prevents ER stress from signaling apoptotic cell death, Nat. Commun. 8 (2017) 1–15, https://doi.org/10.1038/s41467-017-00029-1.
[26] Y. Yang, F. Yang, Z. Xiong, Y. Yan, X. Wang, M. Nishino, D. Mirkovic, J. Nguyen, H. Wang, X.F. Yang, An N-terminal region of translationally controlled tumor protein is required for its antiapoptotic activity, Oncogene 24 (2005) 4778–4788, https://doi.org/10.1038/sj.onc.1208666.
[27] A. Chattopadhyay, D. Pinkaew, H.Q. Doan, R.B. Jacob, S.K. Verma, H. Friedman, A. C. Peterson, M.N. Kuyumcu-Martinez, O.M. McDougal, K. Fujise, Fortilin potentiates the peroxidase activity of Peroxiredoxin-1 and protects against alcohol-induced liver damage in mice, Sci. Rep. 6 (2016) 1–16, https://doi.org/10.1038/srep18701.
[28] R.B. Kapust, J. Tözsér, J.D. Fox, D.E. Anderson, S. Cherry, T.D. Copeland, D. S. Waugh, Tobacco etch virus protease: mechanism of autolysis and rational design of stable mutants with wild-type catalytic proficiency, Protein Eng. 14 (2001) 993–1000, https://doi.org/10.1093/protein/14.12.993.
[29] M. Piotto, V. Saudek, V. Sklenář, Gradient-tailored excitation for single-quantum NMR spectroscopy of aqueous solutions, J. Biomol. NMR 2 (1992) 661–665, https://doi.org/10.1007/BF02192855.
[30] F. Delaglio, S. Grzesiek, G.W. Vuister, G. Zhu, J. Pfeifer, A. Bax, NMRPipe: a multidimensional spectral processing system based on UNIX pipes, J. Biomol. NMR 6 (1995) 277–293, https://doi.org/10.1007/BF00197809.
[31] J.J. Helmus, C.P. Jaroniec, Nmrglue, An open source Python package for the analysis of multidimensional NMR data, J. Biomol. NMR 55 (2013) 355–367, https://doi.org/10.1007/s10858-013-9718-x.
[32] S. Skinner, R. Fogh, W. Boucher, T. Ragan, L. Mureddu, G.J. Vioster, CcpNmr AnalysisAssign: a flexible platform for integrated NMR analysis, Biomol. NMR. 66 (2016) 111–124.
[33] L. Murredu, G. Vuister, Simple high-resolution NMR spectroscopy as a tool in molecular biology, FEBS J. 286 (2019) 2035–2042.
[34] M.P. Williamson, Using chemical shift perturbation to characterise ligand binding, Prog. Nucl. Magn. Reson. Spectrosc. 73 (2013) 1–16, https://doi.org/10.1016/j.pnmrs.2013.02.001.
[35] X. Pu, J.T. Oxford, Proteomic analysis of engineered cartilage, in: Methods Mol. Biol., Clifton, NJ, 2015, pp. 263–278, https://doi.org/10.1007/978-1-4939-2938-2_19.